TECHNICAL REPORT CR-RD-RE-89-1

NEURAL NETWORKS

C. C. Sung
University of Alabama in Huntsville
Department of Physics
Huntsville, AL 35899

and

John L. Johnson
Research Directorate
Research, Development, and Engineering Center

Prepared for:
Research Directorate
Research, Development, and Engineering Center

JANUARY 1990

Contract No. DAAL03-86-0001
(Battelle Columbus Laboratories)

U.S. ARMY MISSILE COMMAND

Redstone Arsenal, Alabama 35898-5000

Approved for public release; distribution is unlimited.

DISPOSITION INSTRUCTIONS

DISCLAIMER

TRADE NAMES

UNCLASSIFIED
SECURITY CLASSIFICATION OF THIS PAGE

REPORT DOCUMENTATION PAGE

Form Approved
OMB No. 0704-0188
Exp. Date Jun 30, 1986

1a. REPORT SECURITY CLASSIFICATION UNCLASSIFIED	1b. RESTRICTIVE MARKINGS
2a. SECURITY CLASSIFICATION AUTHORITY 2b. DECLASSIFICATION / DOWNGRADING SCHEDULE	3. DISTRIBUTION / AVAILABILITY OF REPORT Approved for public release; distribution is unlimited.
4. PERFORMING ORGANIZATION REPORT NUMBER(S)	5. MONITORING ORGANIZATION REPORT NUMBER(S) Technical Report CR-RD-RE-89-1
6a. NAME OF PERFORMING ORGANIZATION Battelle Columbus Laboratories 6b. OFFICE SYMBOL (If applicable)	7a. NAME OF MONITORING ORGANIZATION Research Directorate RD&E Center
6c. ADDRESS (City, State, and ZIP Code) University of Alabama in Huntsville Department of Physics Huntsville, AL 35899	7b. ADDRESS (City, State, and ZIP Code) Commander, U.S. Army Missile Command ATTN: AMSMI-RD-RE-OP Redstone Arsenal, AL 35898-5248
8a. NAME OF FUNDING / SPONSORING ORGANIZATION 8b. OFFICE SYMBOL (If applicable)	9. PROCUREMENT INSTRUMENT IDENTIFICATION NUMBER Contract No. DAAL03-86-D-0001
8c. ADDRESS (City, State, and ZIP Code)	10. SOURCE OF FUNDING NUMBERS PROGRAM ELEMENT NO. / PROJECT NO. / TASK NO. / WORK UNIT ACCESSION NO

11. TITLE (Include Security Classification)
NEURAL NETWORKS

12. PERSONAL AUTHOR(S)
John L. Johnson, and C. C. Sung

13a. TYPE OF REPORT	13b. TIME COVERED	14. DATE OF REPORT (Year, Month, Day)	15. PAGE COUNT
Final	FROM ______ TO ______	JANUARY 1990	53

16. SUPPLEMENTARY NOTATION

17. COSATI CODES			18. SUBJECT TERMS (Continue on reverse if necessary and identify by block number)
FIELD	GROUP	SUB-GROUP	Neural Networks; Optical Architectures; Nonlinear Optics; Adaptation

19. ABSTRACT (Continue on reverse if necessary and identify by block number)

Fundamental properties of neutral networks are discussed and five major models are presented. The emphasis is on the functional interpretation of the describing equations, and includes the nodal activity, learning laws, nonlinear response, stability and overall application areas. Optical implementations by intrinsic nonlinear effects are discussed in detail. Conceptual architectures for the major neural models are presented using optical building blocks for the subsystems. Full concurrent adaptive activity is explicitly included.

20. DISTRIBUTION / AVAILABILITY OF ABSTRACT ☒ UNCLASSIFIED/UNLIMITED ☐ SAME AS RPT. ☐ DTIC USERS	21. ABSTRACT SECURITY CLASSIFICATION UNCLASSIFIED
22a. NAME OF RESPONSIBLE INDIVIDUAL John L. Johnson	22b. TELEPHONE (Include Area Code) 205-876-2650 22c. OFFICE SYMBOL AMSMI-RD-RE-OP

DD FORM 1473, 84 MAR

83 APR edition may be used until exhausted.
All other editions are obsolete.

SECURITY CLASSIFICATION OF THIS PAGE
UNCLASSIFIED

TABLE OF CONTENTS

I. INTRODUCTION

Neural networks are a type of distributed processing system [1]. They consist of a large number of cells, or processing nodes, which are massively interconnected together. The cells receive signals from each other, from other networks or subnetworks, and from the external environment. They generate further signals which are distributed through the networks and to the external environment. The history of neural network modelling and the major concepts are reviewed in references [2] - [8], and the status of the field is examined in [9]. The two major reasons for using neural networks are: first, their intrinsic parallel processing capability; and second, the associative adaptation obtained by varying the strength of the interconnection endpoints according to the current and past activity across the network. The parallel capability opens up a new area of applications to previously unsolvable problems while the adaptation permits the networks to modify their overall behavior to fit the requirements of their environment.

The nodal activity and the strength of the interconnections are the variable parameters treated in the neural models. The interconnection pattern of a neural network is usually considered fixed, and the signal transmission paths are passive (an example of an exception to this is the Grossberg masking field [10].) The pathways introduce, at most, some time delays and attenuation, both of which are neglected in many, but not all, of the major neural models [4].

The output signal of a cell is a positive real scalar quantity. It is the number of pulses per second, averaged over some nominal time, where the pulses are the spike-like bursts emanating from the cell. This is the biological model. No significance has been attached to the spike patterns, but recent research [11,12] indicates that this assumption is not always true. Mathematically, this suggests that the output signal may possess phased subsignals over some basis set, and that future treatments should include complex amplitudes to account for phase, and/or semidigital outputs to account for superpositions of basis functions as being the net signal.

There are many approaches being investigated. Those which attempt to follow the biological models use simple processor rules in the nodes: the inputs are weighted, summed and thresholded to produce the outputs, and the connection strengths are increased on active input channels if the receiving node is also active. This is the generic additive model with a Hebbian learning law [13]. Variations include shunting [14] and error-connection schemes [15,16]. Other approaches are complex programmable nodes with multiple outputs and nonlocal rules, but with relatively few nodes and simple nearest-neighbor interconnects such as the hypercube system consisting of a group of interconnected microprocessors [17].

Despite these numerous variations, there is a major commonality among the models when they are viewed from their functional properties and actual performance. They are parallel, recurrent, adaptive systems. There is no single unified model. Each model is designed to handle a particular type of processing problem (Table 1). A major research issue is simply how to relate the capabilities and performance of various models to actual problems and applications: how, for example, can an optical image be processed so that the objects can be reliably located and identified, or more generally, how can invariant features be extracted from a complex signal distribution?

TABLE 1. Neural network models

Model	Characteristic Use
Adaptive resonance [8]	Hypothesis testing
Back propagation [15]	Supervised learning
BAM, ABAM [13]	Stable adaptation
Crossbar/Hopfield [18]	Optimization
Kohonen [8]	Mapping
Neocognition [8]	Recognition
Boltzman/Cauchy [8]	Optimization
Symbolic substitution [19]	Digital/optical logic
Adaline [16]	Nulling
Perceptron [20]	Nulling
Avalanche [4]	Time sequencing
Shunting [4]	Competitive
Masking fields [10]	Groupings
Counter propagation [8]	Probability mapping
Higher-order learning units [8]	Invariant filters

The functional properties of current neural network models are expressed mathematically as a first-order time derivative of the internal activity of the i^{th} cell set equal to a collection of terms. Each term carries a specific interpretation, and the terms and certain combinations of the terms endow the networks with their functional properties. A neural network model, in general, is described by:

1. A statement of the fixed interconnect matrix.

2. A rule or set of rules describing the nodal activity's temporal behavior and its inputs.

3. A learning law describing how the strength of an interconnection point changes in time.

4. The thresholding function.

5. A stability function.

Since the basic interconnect matrix is fixed, it is rarely discussed as a separate entity. Instead, it is combined with the second and third variables of nodal activity and interconnect strengths, respectively. But for nets which perform fixed logic, [21] for example, the interconnect matrix is the dominant parameter, because in such systems the interconnect strengths are fixed and the nodal signals are flexible. We will be concerned with variable systems, and will not discuss the interconnect matrix in detail.

II. FUNCTIONAL PROPERTIES

The internal activity of the i^{th} cell follows the general dynamical form

$$\frac{da_i}{dt} = \{\text{Loss Term}\} + \{\text{Excitation}\} + \{\text{Inhibitation}\} + \{\text{Adaptation}\}. \quad (1)$$

(While other forms are possible, this is by far the most accepted version.)

The loss term describes a relaxation mechanism leading to the steady state. It is a simple exponential decay:

$$\{\text{Loss Term}\} = - A\, a_i. \quad (2)$$

It can be interpreted as attenuation, absorption, or subtraction. An alternate interpretation is obtained by combining the loss term with the time derivative on the LHS of Eq. (1) and noting that to first order they approximate a_i evaluated at a time $t + (1/A)$. This can be read as a statement of causality, or as indicating a feedback loop with a finite time delay of $1/A$.

The next term is responsible for providing excitation. It can be fixed or adaptive, linear or nonlinear, but its basic feature is that it is a positive and (usually) increasing function of the inputs at a given cell. A somewhat similar term, but with a negative signal provides an inhibitory input. A variation is to use a combined product term where the numerator is designated as the excitation and the denominator is the inhibiting factor which serves as a type of loss as well. Both excitating and inhibiting contributions can be fixed or adaptive. Often, these contributions are in the form of an input signal distribution with a matrix-vector type of connection to the cell. The adaptation is universally assumed in all models to occur by providing a mechanism for varying the strength of the interconnections. The choice of variation, called the learning law, depends on the particular neural network model, since these terms vary in form in different model. Specific discussions are given in the next section.

III. MAJOR MODELS

A. Model Equations

The five most common neural models are the generic additive model, the shunting models, the two-slab bidirectional associative memory (BAM), the back propagation, and the Kohonen model. Their nodal equations are:

1. Generic Additive Model

$$\dot{a}_i = - A\, a_i + I_i + \sum_{j \neq 1} m_{ij}\, S(a_j) \qquad (3)$$

where $S(a_j)$ is the thresholding function and m_{ij} governs the learning law, to be discussed later. I_i is an input signal from the external environment.

2. Shunting Model (Membrane Equation)

$$\dot{a}_i = - A\, a_i + (B - a_i)\, Q_i - (C + a_i)\, P_i \qquad (4)$$

where Q_i is the excitatory input; P_i is the inhibitory input, and A, B, and C are constants.

3. BAM Model (Two Slabs)

$$\dot{a}_i = -A\, a_i + I_i + \sum_{\text{all } j} m_{ij}\, S(b_j) \quad , \tag{5}$$

$$\dot{b}_j = -A\, b_j + J_j + \sum_{\text{all } i} m_{ij}\, S(a_i) \quad . \tag{6}$$

where I_i and J_j are the input signals.

4. Back Propagation

$$a_i^{(n)} = \sum_{\text{all } j} m_{ij}^{(n)}\, S\left(a_j^{(n-1)}\right) \qquad (n^{th} \text{ slab}) \tag{7}$$

5. Kohonen Model

$$a_i = \sum_{\text{all } j} m_{ij}\, I_j \quad . \tag{8}$$

There are several learning laws as well. Most are based on Hebb's observation of pairwise association [22].

B. <u>Learning Laws</u>

The learning laws operate on a much slower time scale than the nodal activity. The most prevalent law is an outer product of the output signal of the i^{th} cell and its j^{th} input signal, with an exponential decay relaxation term [13]. However, some learning laws act on a still larger time scale. For these, each increment of the weight is the steady-state outer product, and these increments are summed over a training cycle time larger than the relaxation time. This is used in the back propagation model, and in the Kohonen model, and is similar to the covariance product sums used in adaptive phased array radar.

Another important variant is the Grossberg competitive law [8] in which the relaxation time is proportional to the output signal strength of the receiving cell.

The major learning laws are:

1. Covariant

$$m_{ij} = S(a_i)\ S(a_j) \quad . \tag{9}$$

2. Hebbian

$$\dot{m}_{ij} = -D\, m_{ij} + S(a_i)\ S(a_j) \tag{10}$$

3. Competitive

$$\dot{m}_{ij} = S(a_i)\left[-m_{ij} + S(a_j)\right] \tag{11}$$

and the Oja variation [23]:

$$\dot{m}_{ij} = S(a_i)\left[-S(a_i)\, m_{ij} + S(a_j)\right] \tag{12}$$

4. Backward Propagation

Error signals $\delta_1^{(n)}$ for n-th path are:

$$\delta_i^{(n)} = S'\left(a_i^{(n)}\right) \sum_{\text{all } j} m_{ij}^{(n+1)} \delta_i^{(n+1)} , \tag{13}$$

$$\Delta m_{ij}^{(n)} = \propto \delta_i^{(n)} S\left(a_j^{(n-1)}\right) , \tag{14}$$

$$\delta_i^{(N)} = S'\left(a_i^{(N)}\right)\left[T_i - S\left(a_i^{(N)}\right)\right] , \tag{15}$$

where N indicates the final output slab; $S' = \dfrac{\partial S(u)}{\partial \mu}$, and T_i is a training signal.

5. Kohonen

$$\Delta m_{ij} = \propto \left(I_i - m_{ij}\right) z_i \tag{16}$$

where $z_i = 1$ if $a_i = \max \{a_k\}$, and is zero otherwise.

C. Thresholding Function

The threshold function describes the formation of a cell's output signal as a function of its internal activity. Early neural models used a linear response, but the current second-generation models are a nonlinear response. This simple innovation is of fundamental importance because it removes the inadequacy of neural networks to provide essential nonlinear learning [24].

Threshold functions:

1. Step Function

$$S(a_i) = \begin{cases} 1, & a_i > 0 \\ 0, & a_i \leq 0 \end{cases} \tag{17}$$

2. "Offset"

$$S(a_i) = \left[a_i\right]^+ = \begin{cases} a_i, & a_i > 0 \\ 0, & a_i \leq 0 \end{cases} \tag{18}$$

3. Hebbian

$$\text{(i)} \quad S(a_i) = \tanh a_i$$

$$\text{(ii)} \quad S(a_i) = \frac{a_i^2}{1 + a_i^2} \quad . \qquad (19)$$

Bias terms and scale factors can be incorporated in the threshold functions.

D. Stability

Another major feature is the stability of a network [25]. It is believed desirable for the network to approach a single optimum state after being given an initial input distribution. Various global quantities with quadratic minima have been defined [1], [16] and used with success to design networks that will produce optimizations in a stable manner. These Lyapunov functions [25], "energy" functions [8], and error functions [1] are of great theoretical interest, but for the purpose of this paper the nodal activity equation and the learning law are adequate guides.

In Equations (1) - (19) the term types are (excluding third rank and higher tensors [30, 31, 32])

a_i	:	linear
$S(a_i)$	:	thresholded
$\sum_j m_{ij} S(a_j)$	:	matrix-vector products

and the operations include multiplication, division, addition, subtraction, differentiation, and integration.

E. <u>Discussion</u>

<u>Description of functions performed by the models</u>

The generic additive model and the two-slab BAM both use the Hebbian learning law. These nets associate inputs because one input distribution is encoded as the interconnects of each node activated by another distribution. Later exposure of either input will reactivate the other input. If part of an input is missing, it will be filled in because the recalled input will, in turn, attempt to reactivate all of the nodes in the first input. Sequences can be encoded on a pairwise basis AB, BC, CD, etc. and superimposed to form an asymmetric memory matrix. Temporal order can be restored either by adjusting the nodal activity time constant or by using a Hebbian learning law which responds to the covariance of the first time derivatives of the nodal output signals (differential

Hebbian). Sequences can be recognized by using an avalanche network: a set of "grandmother" cells (cells tuned to recognize specific patterns) is arranged so that each cell's output excites only the next cell in the sequence. All the cells receive the time-varying input. If the input matches the desired sequence, the corresponding set of cells will reinforce each other in turn, and produce a recognition signal at the end of the sequence. Still other variations are possible. The back propagation and the Kohonen models both incorporate an adaptive fan-out of the input distribution. The Kohonen system self-organizes so that each cell responds best to specific sub-inputs which are closely grouped in the feature space, and thus this model yields good statistical approximations to the overall input distribution. The back propagation model also receives a training input. It forms an error signal as the difference between the actual final output and the training signal of those nodes. This error is propagated back through the interconnect system to form new error signals at every node. The weights are incremented in proportion to the covariance of the errors and the input at each cell. It is a remapping network with good statistical invariance to input signals.

The shunting networks use a variety of learning laws. They are very powerful, general-purpose nets which effectively deal with random and patterned noise, and also automatically renormalize and enhance their activity prior to the slower adaptation processes performing the adaptive encoding.

IV. OPTICAL IMPLEMENTATION

In this section we explain how some of the system equations can be described in an optical system. There are two major problems intrinsic to the project that cannot be easily resolved. The first concerns the identification of the activity a_i with optical quantity, which can be either amplitude or intensity. a_i, being positive in the neural network model, should be interpreted as an intensity which, however, does not appear in optics without manipulation. In other words, the amplitude in optics must be replaced by $[\text{Intensity}]^{1/2}$ and this may or may not be justified. If a_i is considered as an amplitude, a complex quantity, then the phase factor does not admit any interpretation in neural network models. Since this problem cannot be resolved easily and the generalization of a_i as a complex quantity cannot be done at the present time, we will use the slowly varying part of the amplitude in optics as the desired positive number.

Another problem concerns the relaxation time which must be smaller than nanoseconds, whereas in neural networks the time scale is on the order of milliseconds. This difference makes the two systems, neural nets and optical wave equations, never physically equivalent. Again, we can only keep the problem in perspective.

A. Thresholding

The Sigmond function $S(a_i)$ is the output for a given input a_i in the cell. This can be accomplished in several different ways. One method is to take advantage of the amplified medium. Four-wave mixing [26], or a laser amplifier [27] can both achieve this goal. However, all of these methods transfer the energy from external beams to the amplified beam. The disadvantage of setting up the external sources overwhelm whatever advantage that can possibly be gained.

The right choice of nonlinear material can provide a bistable characteristic curve in Fig. 1, where E_{in} and E_{out} are the incoming and

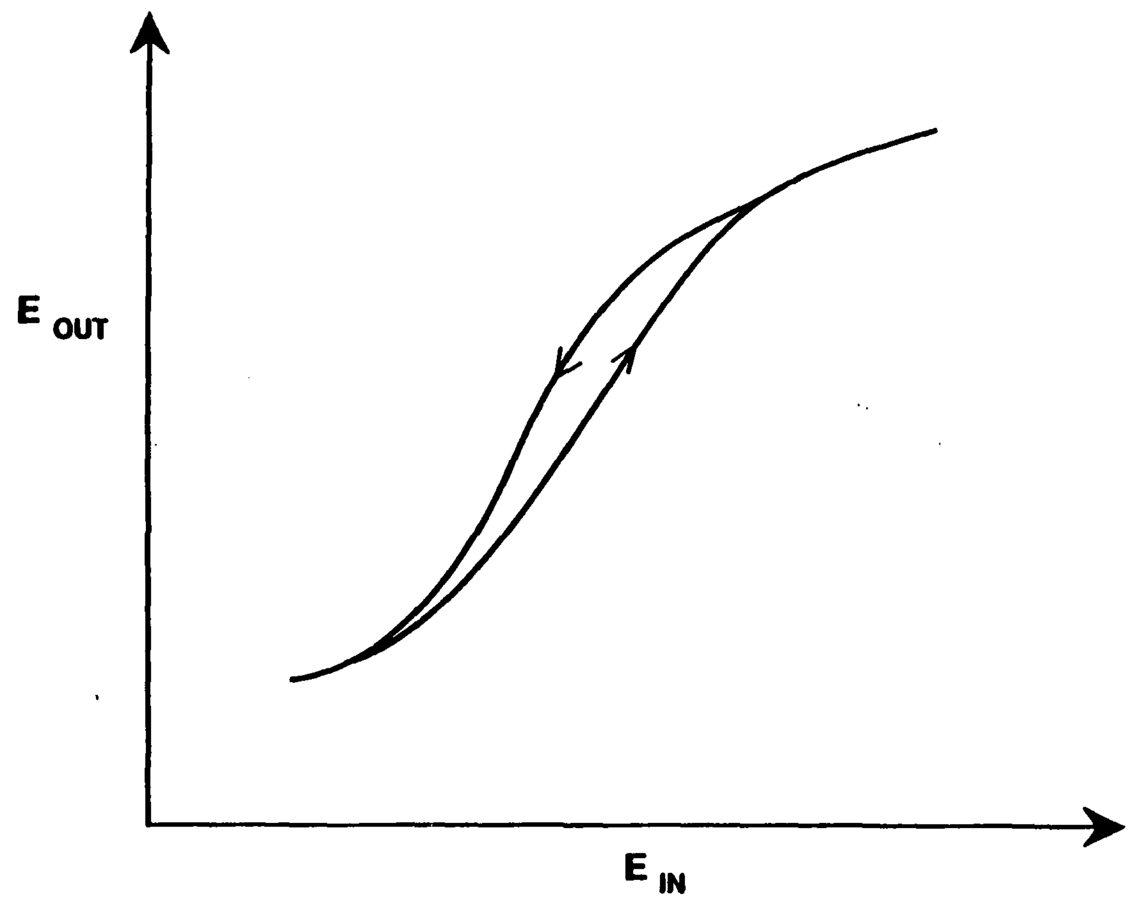

FIGURE 1. CHARACTERISTIC BISTABLE RESPONSE

outgoing amplitudes, respectively. This optical bistable device is easy to set up and a theory can be summarized in one equation (20), [28].

$$\frac{|E_{out}|^2}{|E_{in}|^2} = \left| \frac{4\,(1-r)\sqrt{\epsilon}}{\left[R_+^2\, e^{\alpha'' - i\alpha} - R_-^2\, e^{-\alpha'' + i\alpha}\right]} \right|^2 \tag{20}$$

where

$$R_\pm = \left(1 + \sqrt{r}\right)\sqrt{\epsilon} \pm \left(1 - \sqrt{r}\right) \tag{21}$$

and r is the reflectivity at the medium. The nonlinear part of the dielectric constant ϵ enters through

$$\alpha' + i\alpha'' = \frac{2\pi L}{\lambda}\sqrt{\epsilon} \tag{22}$$

where L/λ is the ratio of the cavity length and wavelength.

Although Eq. (20) is an approximate solution, the accuracy is good enough for our purpose. The next question concerns the material. This subject has been reviewed elsewhere [29]. Many are available depending on the requirement on the thresholding or the switching time. If no strenuous conditions are imposed, then any material with nonlinearity will suffice. In the definition of dielectric constant $\epsilon = \epsilon_\infty + 4\pi X$, and

$$X = X_1 + X_2 E + X_3 \, E \cdot E + \ldots \quad (23)$$

The case where $X_3 \neq 0$ and $X_2 = 0$ defines cubic nonlinear terms. When X_2 is present, the effect of the quadratic nonlinearity frequency doubling, etc. will dominate the desired bistable effect.

We should point out that the nonlinear optical material considered here and the photorefractive material used later can both perform the thresholding of this section, and the association memory of the next section . The reason for adoption of the usual nonlinear bistable material described in Eq. (20), for example, GaAs, CdS, etc. for thresholding while associative memory is considered along with the photorefractive material like $BaTiO_3$, etc. is a matter of convenience for practical purposes. For example, it has been reported [30] that GaAs can perform the four-wave mixing just as well as the photorefractive material, with vastly improved speed at the expense of a much larger required intensity. In this report we follow the conventional application in the literature.

B. Adaptive Term and Photorefractive Medium

The index of refraction of a photorefractive material can be written as

$$n = n_o + n_a e^{i\varphi_a} \left(A_1^* A_4 + A_2 A_3^* \right) \exp ik_a \cdot r + c.c.$$
$$+ n_b e^{i\varphi_b} \left(A_1 A_3^* + A_2 A_4^* \right) \exp ik_b \cdot r + c.c.$$
$$+ n_c e^{i\varphi_c} A_1 A_2^* \exp ik_c \cdot r + c.c.$$
$$+ n_d e^{i\varphi_d} A_3^* A_4 \exp ik_d \cdot r + c.c. \qquad (24)$$

where n_a ... n_d etc. are the optical nonlinearities and φ_a ... φ_d are constants. Equation (24) is simply the index of refraction according to the cubic nonlinearity with the specific conditions due to the arrangement

$$\vec{k}_1 - \vec{k}_4 = -\vec{k}_2 + \vec{k}_3 \equiv \vec{k}_a \left(k_1 = -k_2 , k_3 = -k_4 \right) \qquad (25)$$

$$\vec{k}_1 = -\vec{k}_3 = \vec{k}_2 - \vec{k}_4 \equiv \vec{k}_b \ . \qquad (26)$$

When n is substituted into the Maxwell equation and each component of $\exp ik_i x$ $(i=1,2,3,4)$ is identified, we obtain [26]

$$\left(\frac{\partial}{\partial z} + \frac{1}{c}\frac{\partial}{\partial t}\right)A_1 = Q_1A_4 - Q_2A_3 - Q_3A_2 \tag{27a}$$

$$\left(\frac{\partial}{\partial z} - \frac{1}{c}\frac{\partial}{\partial t}\right)A_2 = Q_1^*A_3 - Q_2^*A_4 - Q_3^*A_1 \tag{27b}$$

$$\left(\frac{\partial}{\partial z} - \frac{1}{c}\frac{\partial}{\partial t}\right)a_3 = - Q_1 A_2 - Q_2^* A_1 - Q_4 A_4 \tag{27c}$$

$$\left(\frac{\partial}{\partial z} + \frac{1}{c}\frac{\partial}{\partial t}\right)A_4 = - Q_1^* A_1 - Q_2 A_2 - Q_4^* A_3 \tag{27d}$$

where Q_i $(i=1,2,3,4)$ obey the Debye equations

$$\gamma_1\dot{Q}_1 + Q_1 = \frac{\gamma_1}{I_0}\left(A_1A_4^* + A_2^*A_3\right) \tag{28a}$$

$$\gamma_2\dot{Q}_2 + Q_2 = \frac{\gamma_2}{I_0}\left(A_1A_3^* + A_2^*A_4\right) \tag{28b}$$

$$\gamma_3 \dot{Q}_3 + Q_3 = \frac{\gamma_3}{I_0}\left(A_1 A_2^*\right) \tag{28c}$$

$$\gamma_4 \dot{Q}_4 + Q_4 = \frac{\gamma_4}{I_0}\left(A_3 A_4^*\right) . \tag{28d}$$

and $I_0 = \Sigma\, I_i = \Sigma\, |A_i|^2$.

Notice that the Maxwell equations imply $\dot{Q}_i = 0$. In Eq. (28) the $\dot{Q}_i$ factor is often introduced, as is done here, to reflect the buildup time of a hologram from various beams in the medium. Equations (27) - (28) look very similar to the BAM model but with some important differences. First is the use of complex numbers introduced throughout the formalism. The phase factor is crucial in optics although the corresponding network activity a_i are supposed to be real. Another factor is the difference between a_i and $S(a_i)$ that must be addressed by means of thresholding. In view of these difficulties, we cannot take this set of equations and try to identify them as a part of BAM. The photorefractive interference, as discussed however, will be used as a "component" of the BAM to function or perform as the adaptive term. This is to be illustrated in the next section.

We follow here one example set up by Yariv et al. [31] The pump beam in Fig. 2 is to be identified as $S(a_i)$ and $S^*(b_j)$. Then the nonlinear part of the index of refraction is

$$\Delta n = \sum_{ij} S^*(a_i) \; S(b_j) \cdot A_{ij} \tag{29}$$

where

$$A_{ij} \propto e^{+i\left(\vec{k}_a - \vec{k}_b\right) \cdot \vec{r}} \tag{30}$$

and Δn is stored in a hologram. When E' in the <u>direction</u> of $S(a)$ shines on the hologram, then a diffraction beam E_{diff}

$$E_{diff} = J \; e^{-\vec{k}_b \cdot \vec{r}} \tag{31}$$

is produced, and

$$J = \int E'(r') \, S^*(a_i) \; S(b_j) \; d^3r' \exp\left\{ik\left(xx' + yy'\right)/r\right\}$$

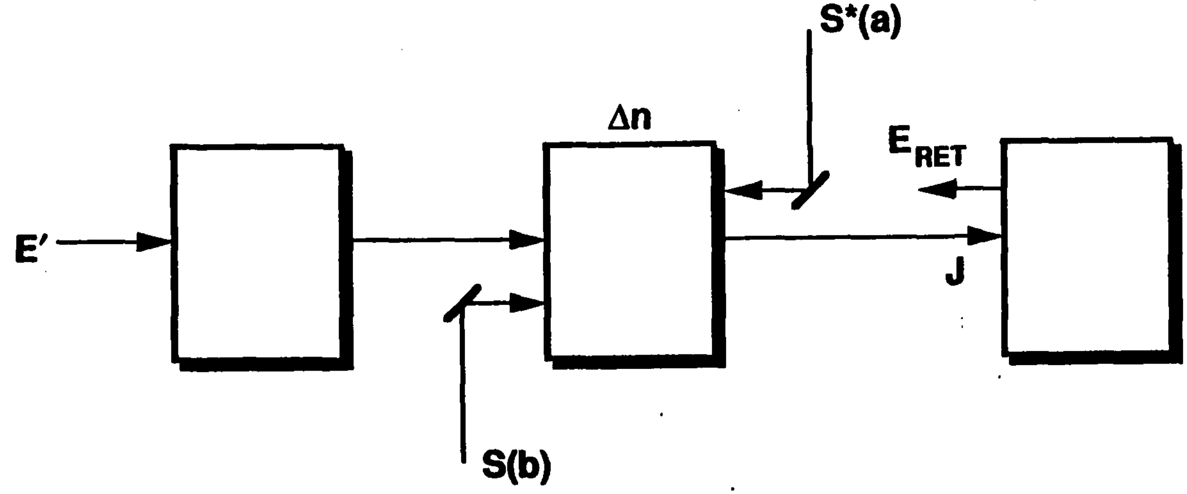

FIGURE 2. PHOTOREFRACTIVE BEAM GEOMETRY FOR ASSOCAITIVE ENCODING.

is the overlapping integral. The reflected field moves opposite to $S(b_j)$ $\propto$ $S^*(a)\, S(b)$, and this reflected beam excites Δn again to produce a field proportional to

$$\Delta n\, E_{out} = J\, |S(b_j)|^2\, S^*(a) \quad . \tag{32}$$

The net result, if all contributions are considered, can be expressed as

$$(\Delta E)_i = \sum_j{}' m_{ij}\, S(b_j) \tag{33}$$

and

$$\Gamma \dot{m}_{ij} + m_{ij} = S^*(a)\; S(b) \; . \tag{34}$$

In actuality, $m_{ij} \propto S^*(a)\, S(b)$, but the time derivative in Eq. (34) is added to reflect the time delay between $S^*(a)$ and $S(b)$ turn-on and the production of $(\Delta E)_i$. Equations (33) and (34) for $(\Delta E)_i$ show how the adaptive term can be produced with the output proportional to J , the overlapping integral. This scheme has the advantage for application of training and learning, i.e., the stored information Δn is retrieved by the incident wave E_i.

For our purpose of demonstration of the adaptive term in BAM, a simpler setup can be given as follows. The holograph is set up as

$$\Delta n = \sum S^{*}(a_i)_p \ S(b_j)_p \tag{35}$$

by two pump beams. A probe beam $S^{*}(b_j)$ is then refracted from the diffraction grating to produce the conjugate beam $(\Delta S(a_j))_c$.

Or, in our notation,

$$\left(\Delta S(a_i)\right)_c = \sum m_{ij} S^{*}(b_j) \tag{36}$$

and

$$\Gamma\left(\dot{m}_{ij}\right) + m_{ij} = S^{*}(a_i) \ S(b_j) \tag{37}$$

Again, the time derivative is added for consideration of buildup time for the diffracting.

A short summary of discussion is given here. We demonstrate how an optical beam called $(\Delta S(a))_c$ can be produced for a given set of (a_i, b_j) as shown in Fig. 3, when $b_j \rightarrow S(b_j)$, $a_i \rightarrow S(a_i)$ by the thresholding processes. $(S(a_i))_c$ then is numerically equal to $\Sigma_j m_{ij} S(b_j)$ with m_{ij} defined in Eq. (37).

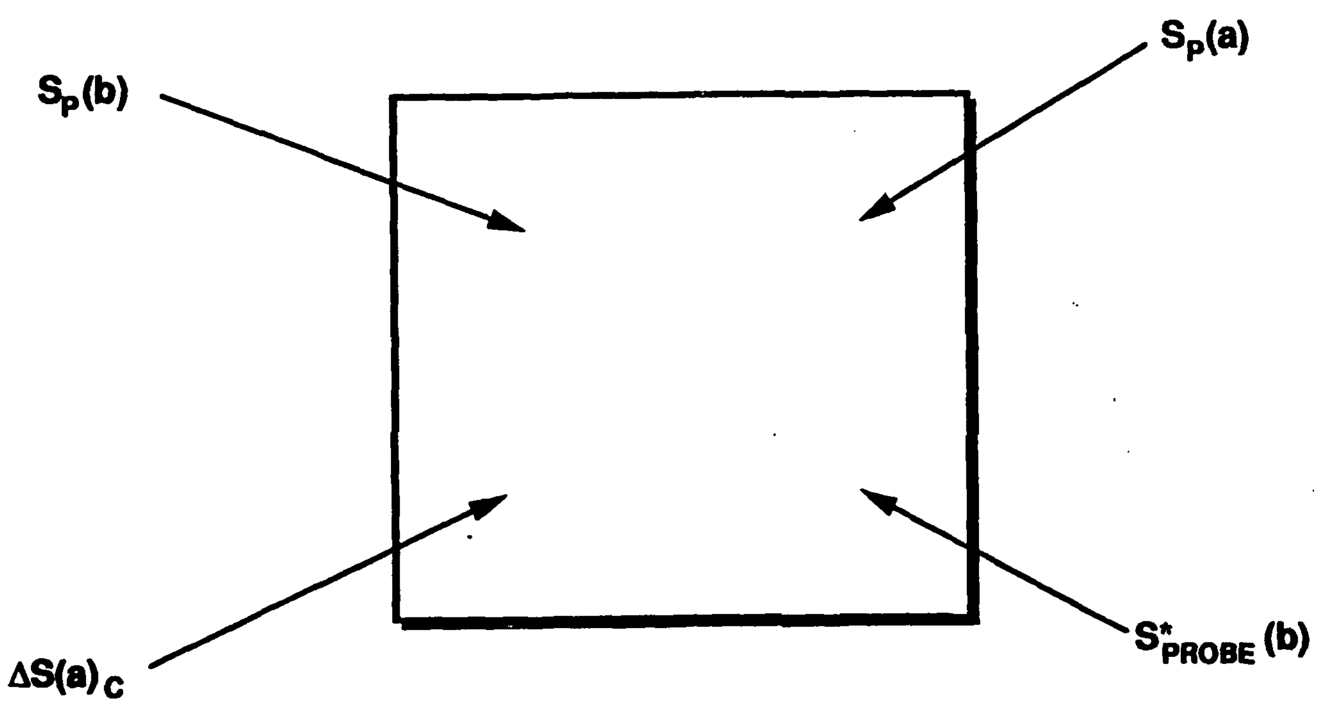

FIGURE 3. PHOTOREFRACTIVE BEAM GEOMETRY FOR ASSOCIATIVE RECALL.

A major point to be made is that currently the only optical effect which has been found useful for implementing associative memories is the photorefractive effect. There is no other way to do it without going to hybrid systems.

C. Shunting Mechanism

The shunting term is of the form given by

$$a_i \sum_j S(a_j)$$

which is proportional to the product of the two amplitudes a_i and $S(a_j)$ in contrast to the triple product for the adaptive case. It seems one should be able to use the X_2 term to generate this term. This cannot be carried out because this nonlinear term has its dominant effect on the phase in the wave propagation and not on the absolute magnitude of the amplitude.

We have examined the technique of optical correlation in the literature and found that our need is much simpler, since no spatial information is contained in a_i. To accomplish the shunting term we use the geometry in Figure 4 where a photorefractive crystal is present, and

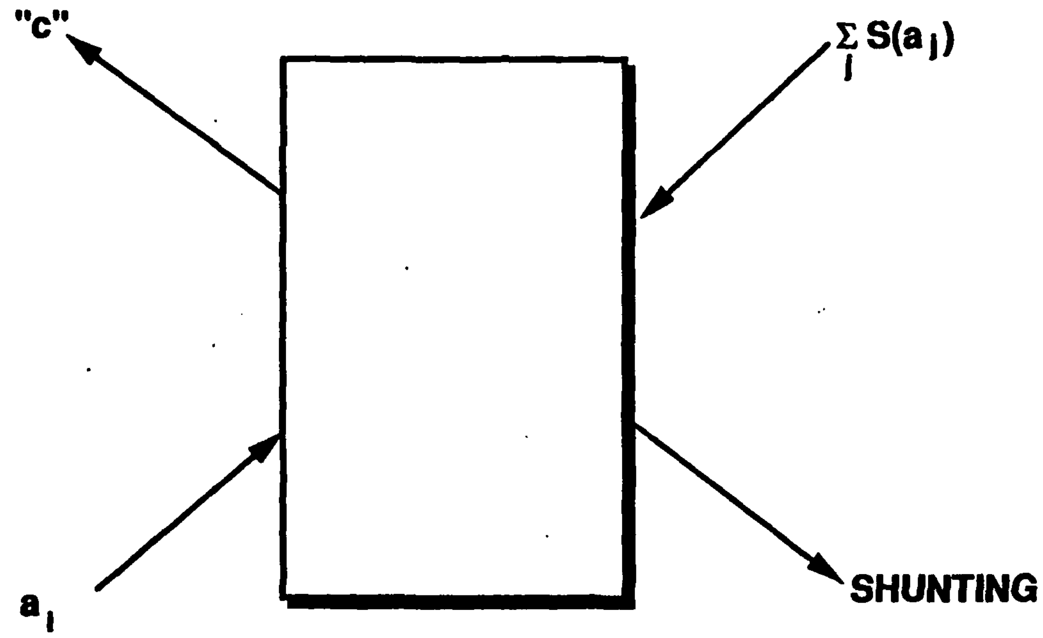

FIGURE 4. SHUNTING BEAM GEOMETRY.

the two pump beams a_i and $\Sigma_j S(a_j)$ form a grating according to the shunting term

$$\Delta n = \gamma \sum_j a_i S(a_j) e^{i\left(\vec{k}_i - \vec{k}_j\right) \cdot \vec{r}} . \tag{38}$$

Then a beam of constant amplitude $c e^{i\vec{k}_c \cdot \vec{r}}$ will be scattered from Δn, with the resultant amplitude proportional to A_c :

$$A_c \propto c \sum_j a_i S(a_j) e^{i\left(\vec{k}_i - \vec{k}_j - \vec{k}_c\right) \cdot \vec{r}} . \tag{39}$$

We note that this term is just the shunting amplitude with specific direction $(\vec{k}_i - \vec{k}_j - \vec{k}_c)$.

D. Amplification

When the optical system is designed, absorption in the system, intrinsic or external, cannot be avoided. At certain stages of operation the optical amplitude must be amplified to sustain the operation. Four-wave mixing in a nonlinear medium can accomplish this goal.

E_1 and E_2 in the diagram of Fig. 5 are the pump beams. E_4 is the conjugated beam at $z = L_1$ and E_3 is the probe beam, which satisfy

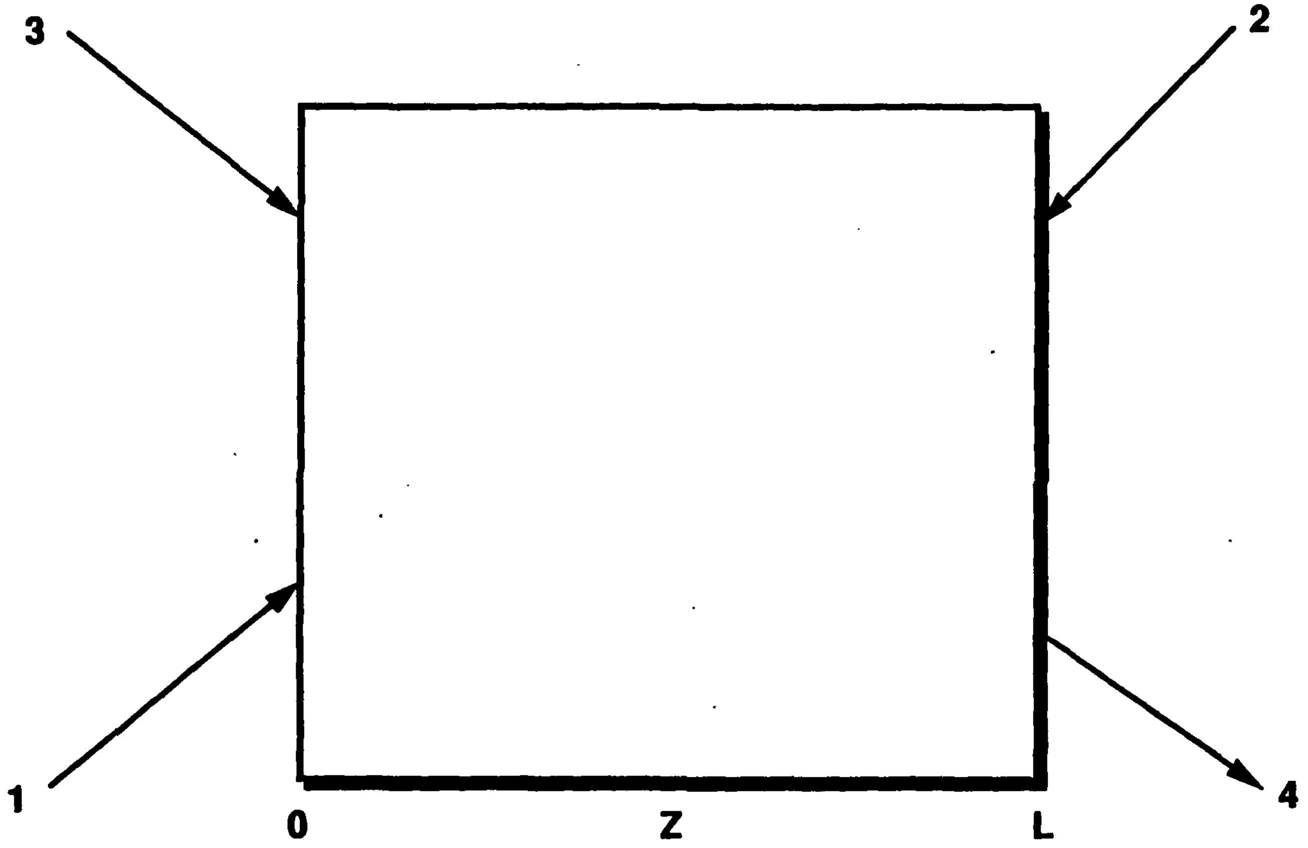

FIGURE 5. NONLINEAR BEAM AMPLIFICATION GEOMETRY.

$$\left|\frac{E_4}{E_3}\right|^2 = \frac{(\sin \mu L)^2}{\left(\frac{\mu}{\chi}\cos \mu L\right)^2 + \left(\frac{\Delta k}{2\chi}\sin \mu L\right)^2} \tag{40}$$

where

$$\mu = \sqrt{(\gamma E_1 E_2)^2 + (\Delta k/2)^2} \tag{41}$$

$$\chi = |\gamma E_1 E| \; ,$$

where γ is the coupling constant and $\Delta k = |\vec{k}_1 + \vec{k}_2 - \vec{k}_3 - \vec{k}_4|$ is the phase mismatching, which in general is zero. Consequently, E_4/E_3 can take almost any value when $\Delta kL << 1$.

In summary, we have demonstrated the optical elements performing the following tasks for a <u>given</u> set of (a_i, b_j):

(1) Thresholding to convert

$$a_i \rightarrow S(a_i)\; , \quad b_j \rightarrow S(b_j)$$

(2) Production of neural adaptive changes

$$\Delta = \Sigma\, m_{ij}\; S(b_j)$$

where

$$\dot{m}_{ij} + \Gamma m_{ij} = S(a_i)\; S^*(b_j)\; .$$

(3) Performing the shunting as dictated by

$$a_i \sum_j S(a_j)$$

(4) Producing the amplified signal, which is accomplished by integrating all elements as described in this section.

V. CANDIDATE IMPLEMENTATIONS OF THE NEURAL NETWORKS

A. Conceptual Architectures for Optical Neural Networks

The objective of this section is to devise candidate implementations of the neural networks discussed in the first section using the optical effects discussed in the second section. Where possible, all-optical architectures are chosen that do not have detector arrays and electronically converted video data. However, some hybrid techniques have been used where they appeared to be the only method available.

B. Building Blocks

The photorefractive effect has been used as the preferred method for associative memory. The usual approach of storing a hologram made from the mutual interference of two input images suffers the drawbacks of low output during recall. This is because the output is a diffracted reconstruction. An elegant solution which provides full-strength reconstruction has been shown by Stoll and Lee, and their technique will be used here. Basically, their system consists of a cascaded pair of matched filter correlators whcih encode given pairs of images by multiplying them with a different reference angle for each pair. Thus a given reference beam exits between the matched filters, and it is amplified by a nonlinear crystal prior to its reading of the second matched filter.

Their system has a fundamental difficulty that prevents its use as a fully adaptive optical associative system: The associative encoding process and the ensuing readout process are performed separately. Thus the encoding activity does not account for the modification of the output signals as the associative matrix is formed. This is a problem found with almost all adaptive associative systems using the photorefractive effect. It can be resolved by use of polarization-switching dynamic volume holograms as first shown by Psaltis [8]. By combining the Psaltis technique with Stoll and Lee's system, an adaptive optical associative architecture can be devised and is shown in Figure 6. Its operation is as follows: Two photorefractive crystals A with a gain crystal B are arranged in the Stoll and Lee configuration with a reference beam θ

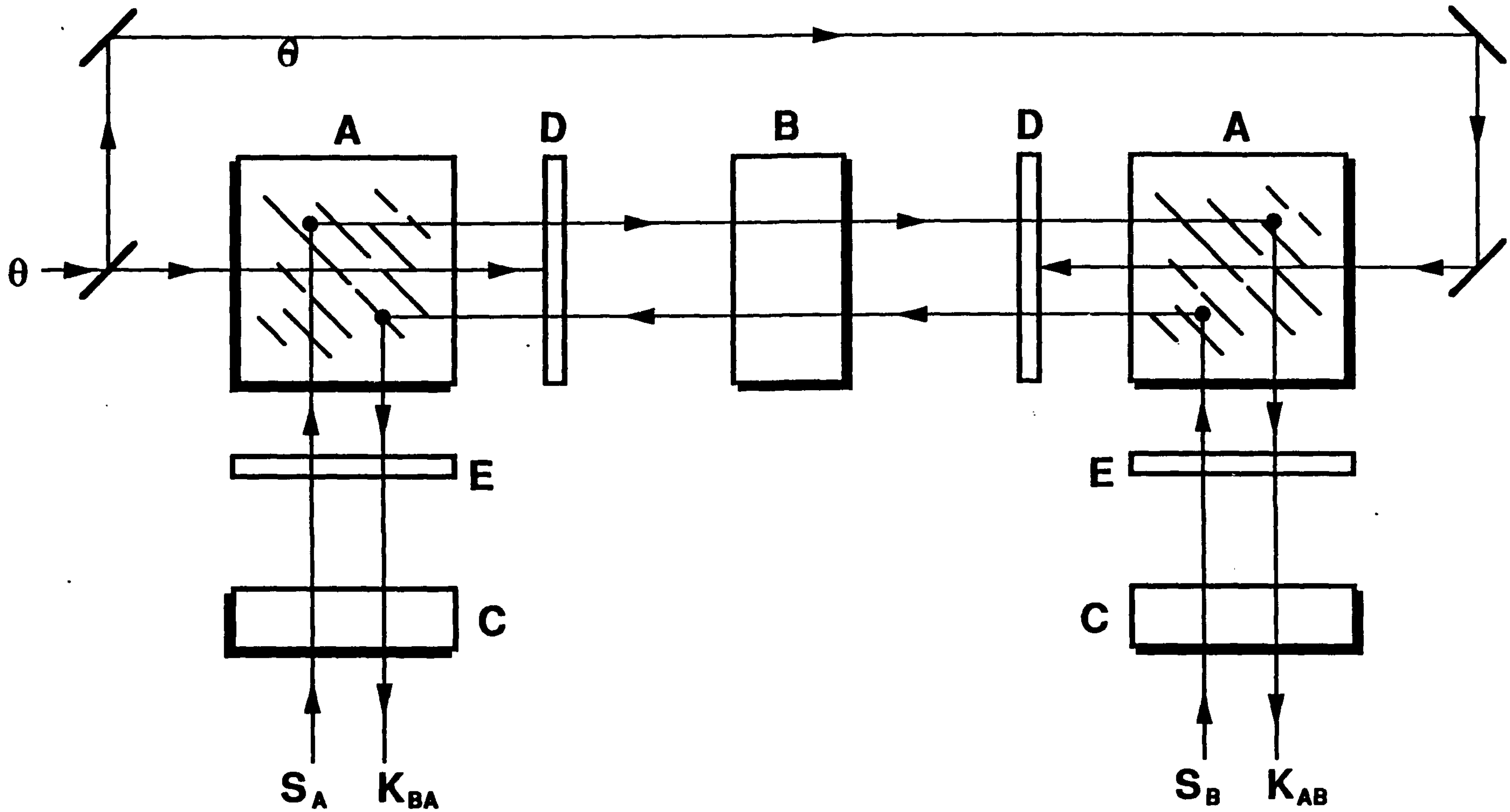

FIGURE 6. ASSOCIATIVE OPTICS

being provided to each crystal A . The input distributions S_A and S_B to be associated pass through nonreciprocal Faraday rotaters C as in the Psaltis system. Θ has a polarization at 90°. S_A and S_B are placed at -45°. The rotaters C produce a +45° rotation to S_A and S_B so that when they enter the photorefractive crystals A they are also polarized at 90°. They interfere with the Θ-beam to produce the desired volume holograms in the crystals A . As the holograms form, S_A and S_B are diffracted from them. The diffracted beams, due to the large angles between the S_A , S_B and Θ beams, are polarization-switched to the orthogonal 0° polarization state as in the Psaltis arrangement of Reference 8. These diffracted beams pass through the gain crystal B and are incident upon the photorefractive crystals again, where they contact with the volume holograms and are again diffracted to form the output beams K_{BA} and K_{AB} . These beams also undergo polarization-switching from 0° to 90°. They pass through the rotations C and emerge at a polarization angle of +45°, orthogonal to the S_A and S_B beams. They can then be separated by a polarizing beamsplitter. They are the adaptive inputs to the slabs generating the signals S_A and S_B . Thus the adaptive contributions are available during the encoding process. After the system reaches equilibrium, new pairs of slab inputs (not shown) can be presented with the angular reference beam θ reset to a new angle.

The remaining building blocks are less complex. Figure 7 shows the threshold crystal. It can be a bistable device, or a pumped $BaTiO_3$ operating in the saturation regime. Figure 8 shows how an optical feedback loop provides the necessary time delay factor to generate the loss term in the nodal activity. Shunting can be achieved by the technique discussed earlier, or a hybrid implementation used in which a SLM is inserted into the time delay loop to vary the splitting coefficient k in proportion to the local average of the slab activity.

With these building blocks, the following optical architectures can be schematically developed for the additive, BAM, and backpropagation nets. Inspection of the defining equations for the BAM and additive models shows that they are basically equivalent if we set $I = J$. Accordingly, only the BAM architecture is discussed here. It is shown in Figure 9. It consists of the adaptive building block with provisions for adding the

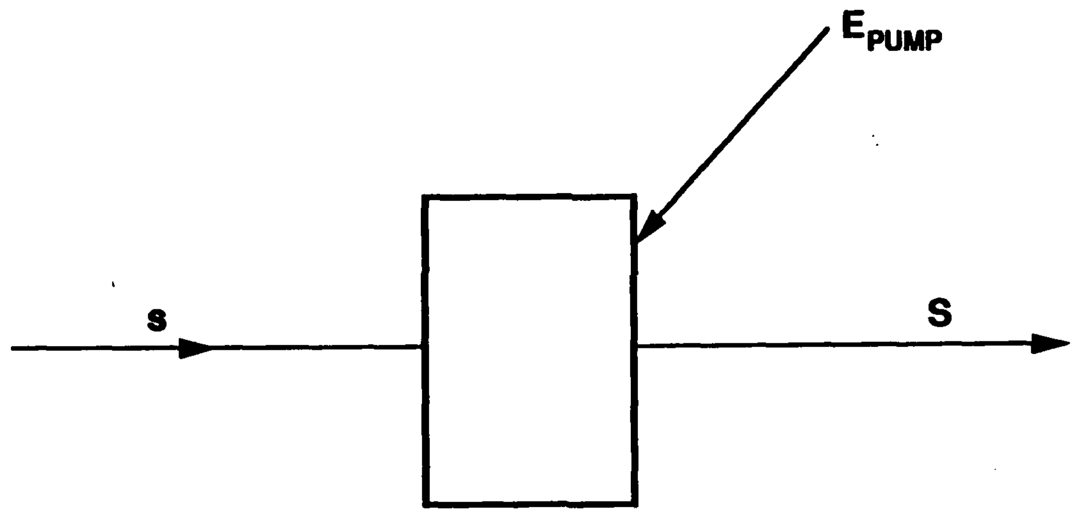

FIGURE 7. THRESHOLD OPTICS

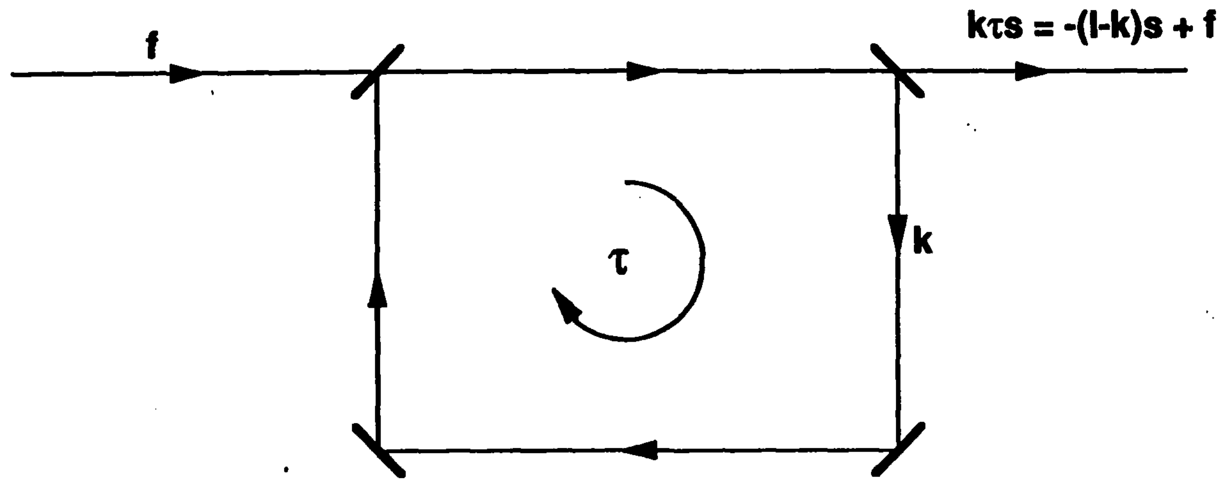

FIGURE 8. TIME DELAY LOOP

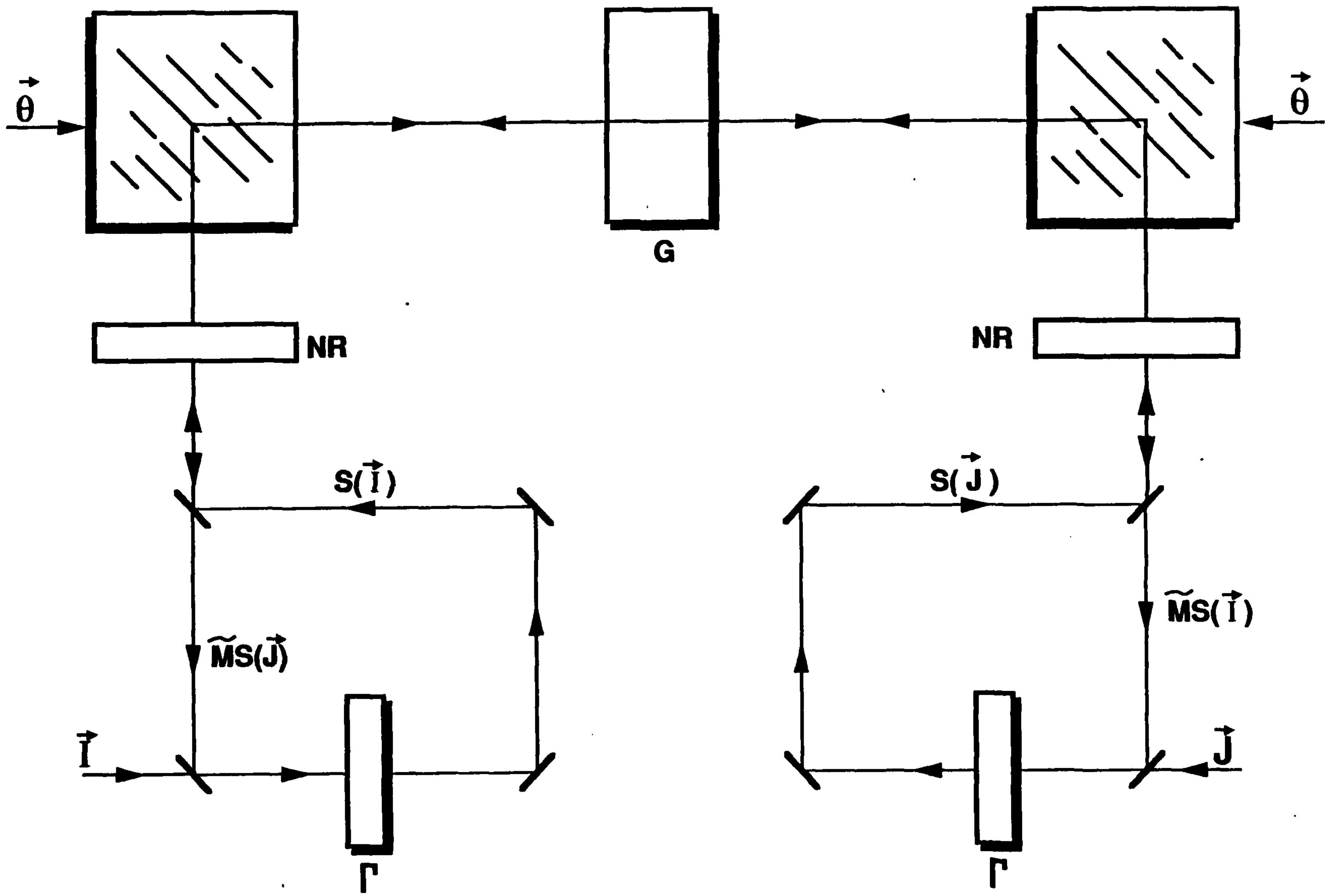

FIGURE 9. BAM MODEL (FOR ADDITIVE, $\vec{I} = \vec{J}$)

input distributions to the adaptive terms and thresholding the run. This is done in the loops shown below the adaptive optics.

The backpropagation architecture is more complex and requires additional explanation. It is shown in Figure 10. Two adaptive systems are arranged in a square. Two additional photorefractive crystals A and two more thresholding crystals B are used. The new thresholding crystals are operated so that an incident beam will be turned off rather than on at the threshold. Their threshold level is higher than the regular threshold crystals Γ. The crystals A form a grating proportional to the product of their inputs. Their inputs are in turn diffracted from this grating. The diffracted S' beam, containing the square of S' rather than S' itself, is used as an approximation to the exact form from backpropagation theory. While cumbersome, this architecture satisfies all the basic requirements of an optical implementation of the standard three-layer feedforward backpropagation algorithm.

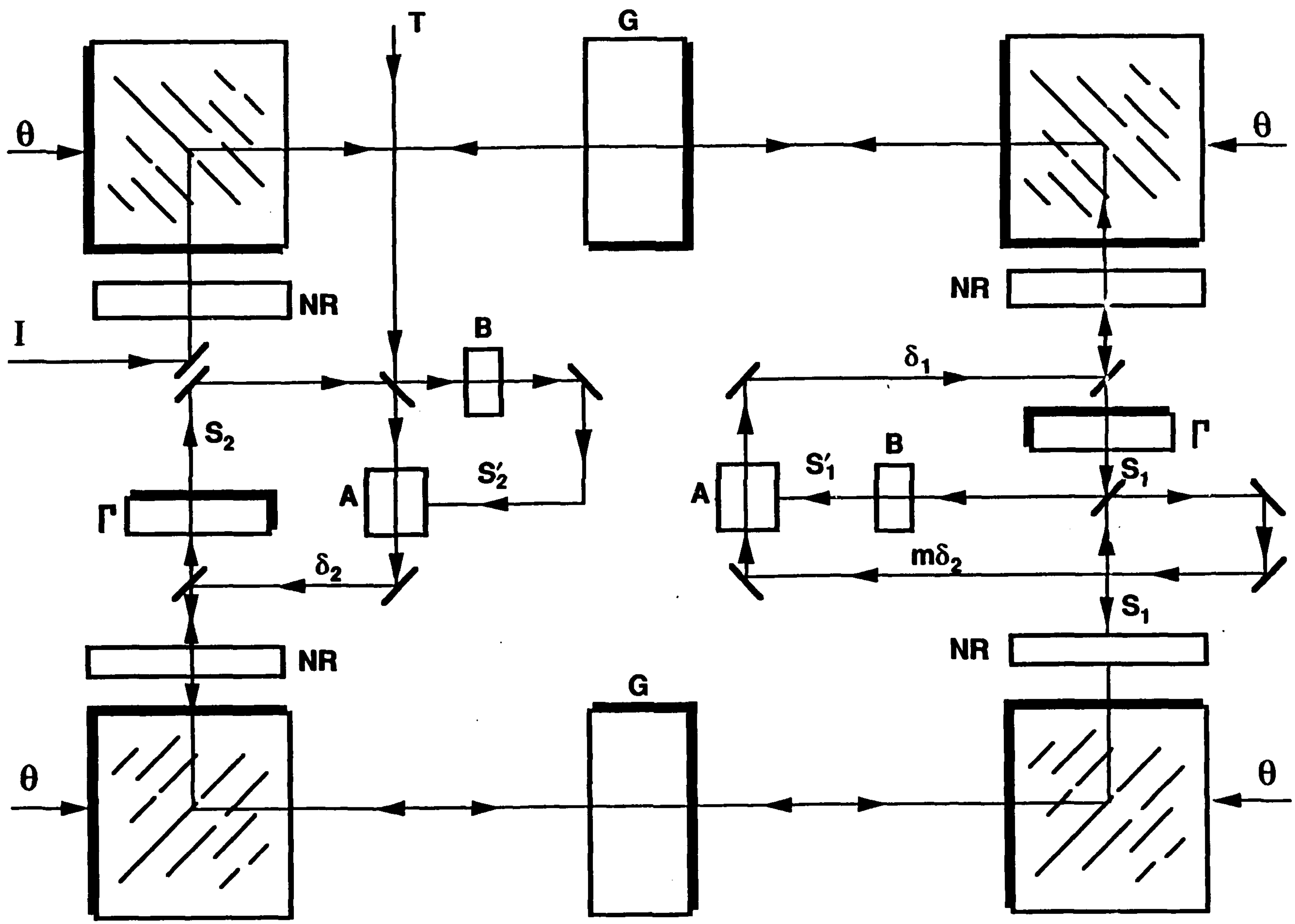

FIGURE 10. BACKPROPAGATION OPTICS

REFERENCES

1. Rumelhart, D. E., McClelland, J. L., et al., Parallel Distributed Processing, MIT Press, Cambridge, MA (1986).

2. Grossberg, S., "Recent Developments in the Design of Real-Time Nonlinear Neural Network Architectures", Proc. IEEE First International Conference on Neural Networks, IEEE Catalog No. 87TH0191-7, June 21-24, 1987, Vol. 1.

3. Kohonen, T., "State of the Art in Neural Computing", Proc. IEEE First International Conference on Neural Networks, IEEE Catalog No. 87TH0191-7, June 21-24, 1987, Vol. 1.

4. Grossberg, S., Studies of Mind and Brain, Boston Studies in the Philosophy of Science, Vol. 70 (Reidel, Norwell, MA, 1982).

5. Kohonen, T., "An Introduction to Neural Computing", Neural Networks, Vol. 1, No. 1, 1988.

6. Grossberg, S., "Nonlinear Neural Networks: Principles, Mechanisms, and Architectures", Neural Networks, Vol. 1, No. 1, 1988.

7. Hestenes, D., "How the Brain Works: The Next Great Scientific Revolution", 3rd Workshop on Maximum Entropy and Bayesian Methods in Applied Statistics, University of Wyoming, August 1-4, 1983.

8. Applied Optics, entire issue devoted to neural networks, Vol. 26, No. 23, 1 Dec 1987.

9. DARPA Neural Network Study - available from MIT Lincoln Lab, ATTN: Distribution Office, P.O. Box 73, Lexington, MA 02173 (1988).

10. Cohen, M. A. and Grossberg, S., "Masking Fields: A Massively Parallel Neural Architecture for Learning, Recognizing, and Predicting Multiple Groups of Patterned Data", Appl. Opt., Vol. 26, No. 10, 15 May 1987.

11. Vaughan, C., "A New View of Vision", Science News, Vol. 134, 23 July 1988.

12. Dayhoff, J. E., "Detection of Favored Patterns in the Temporal Structure of Nerve Cell Connections", Proc. IEEE First International Conference on Neural Networks, IEEE Catalog No. 87TH0191-7, June 21-24, 1987, Vol. III.

13. Kosko, B., "Sampling Adaptive Bidirectional Associative Memories", Proc. 21st Asilomar Conf. on Signals, Systems, and Computers, Nov 1987.

14. Reference 4, Chapt. 1.

15. Werbos, P., Beyond Regression: New Tools for Prediction and Analysis in Behavioral Sciences. Doctoral thesis and published report. Harvard University, Cambridge, MA, (1975).

16. Widrow, B. and Hoff, M. E., "Adaptive Switching Circuits", 1960 WESCON Convention, Record Part IV (1960).

17. Barhen, J., et al., "Optimization of the Computational Load of a Hypercube Supercomputer Onboard a Mobile Robot", Appl. Opt., Vol. 26, No. 23, 1 Dec 1987.

18. Hopfield, J. J., "Neural Networks and Physical Systems with Emergent Collective Computational Abilities", Proc. Natl. Acad. Sci. U.S.A. 79, 2554 (1982).

19. Huang, A., "Parallel Algorithms for Optical Digital Computers", Proc. IEEE 13 (1983).

20. Rosenblatt, F., "The Perceptron: A Probabilistic Model for Information Storage and Organization in the Brain", Psych. Rev. 65, 386 (1958).

21. Johnson, J. L., "Architectural Relationships Involving Symbolic Substitution", Appl. Opt., Vol. 27, No. 3, 1 Feb 1988.

22. Hebb, D., Organization of Behavior, (Wiley, NY, 1949).

23. Levy, W. B. and Burger, B., "Electrophysiological Observations Which Help Describe an Associative Synaptic Modification Rule", Proc. IEEE First International Conference on Neural Networks, IEEE Catalog No. 87TH0191-7, June 21-24, 1987, Vol. IV.

24. Minsky, M. L. and Papert, S., Perceptrons (MIT Press, Cambridge, MA, 1969).

25. Cohen, M. A. and Grossberg, S., "Absolute Stability of Global Pattern Formation and Parallel Memory Storage by Competitive Neural Networks", IEEE Trans. Syst. Man. Cybern SMC-13, 815 (1983).

26. "Optical Phase Conjugation" edited by R. A. Fisher (1983), Academic Press.

27. A. Yariv, "Quantum Electronics", John Wilye and Sons, NY (1975).

28. C. C. Sung and C. M. Bowden, J. Opt. Soc. Am. B1, 395 (1984).

29. H. M. Gibbs, Optical Bistability, Academic Press, (1985).

30. Optical Bistability 2, edited by C. M. Bowden, H. M. Gibbs, and S. L. McCall, Plenum Press, NY, (1984).

31. S. K. Kavong, Kyuma, A. Yariv, Appl. Phys. Lett. 48, 1114 (1986).

INITIAL DISTRIBUTION

	Copies
Director U.S. Army Research Office SLCRO-PH SLCRO-ZC P.O. Box 12211 Research Triangle Park, NC 27709-2211	2
Headquarters Department of the Army DAMA-ARR Washington, DC 20310-0632	1
Headquarters OUSDR&E ATTN: Dr. Ted Berlincourt The Pentagon Washington, DC 20310-0632	1
Defense Advanced Research Projects Agency Defense Sciences Office Electronics Systems Division ATTN: Andrew Yang 1400 Wilson Boulevard Arlington, VA 22209	1
Commander U.S. Army Foreign Science & Technology Center AIAST-RA 220 Seventh Street NE. Charlottesville, VA 22901-5396	1
Commander U.S. Army Strategic Defense Command DASD-H-V P.O. Box 1500 Huntsville, AL 35807-3801	1
Director, URI University of Rochester College of Engineering and Applied Science The Institute of Optics Rochester, NY 14627	1
Director, JSOP University of Arizona Optical Science Center Tucson, AZ 85721	1

INITIAL DISTRIBUTION

		Copies
US Army Materiel System Analysis Activity ATTN: AMXSY-MP Aberdeen Proving Ground, MD 21005		1
IIT Research Institute ATTN: GACIAC 10W. 35th Street Chicago, IL 60616		1
AMSMI-RD,	Dr. McCorkle Dr. Rhoades Dr. Stephens	1
AMSMI-RD-RE,	Mr. B. Jennings	1
	Dr. J. Bennett	1
AMSMI-RD-OP,	Dr. J. Johnson	30
AMSMI-RD-CS-R		15
AMSMI-RD-CS-T		1
AMSMI-GC-IP,	Mr. Fred Bush	1